# Raman O VI Spectroscopy and Polarimetry of Asymmetric Accretion Flows in Symbiotic Stars

**Hee-Won Lee**

**In Collaboration with Jeong-Eun Heo, Seok-Jun Chang, Young-Min Lee**
**R. Angeloni, F. Di Mille, T. Palma**

**Sejong University**
**2016 December 5**

# Contents

# INTRODUCTION - PROGENITORS OF TYPE IA SUPERNOVAE?

1. Accelerated expansion using Type Ia supernovae
2. Accretion onto a white dwarf from a mass losing companion.
3. Reaching the Chandrasekhar limit, a supernova explosion takes place.
4. Cataclysmic variable vs. Symbiotic stars

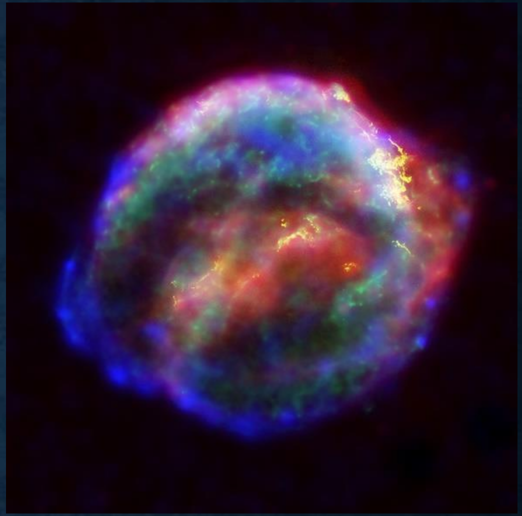

Kepler SN, HST

SN1994D, NGC4526, HST

# Introduction – Symbiotic stars

1. Spectra characterized by a hot component, a cool component and various emission lines.
2. The cool component is a mass losing giant.
3. The hot component is usually a white dwarf.
4. Various activities can be attributed to wind accretion.
5. O VI 1032 and 1038 are very strong.
6. Classified into ‘S’ and ‘D’ type symbiotic stars.
7. S type symbiotics show orbital periods ranging in several hundred days, whereas D type symbiotics may exceed a decade.

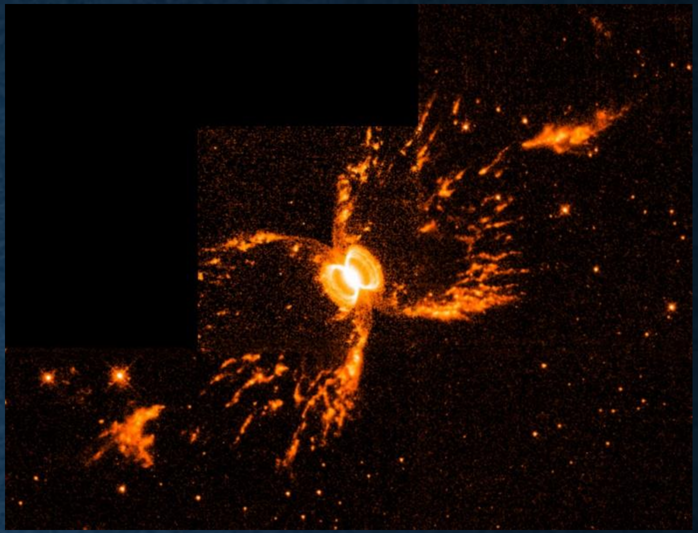

Southern Crab (Corradi, HST)

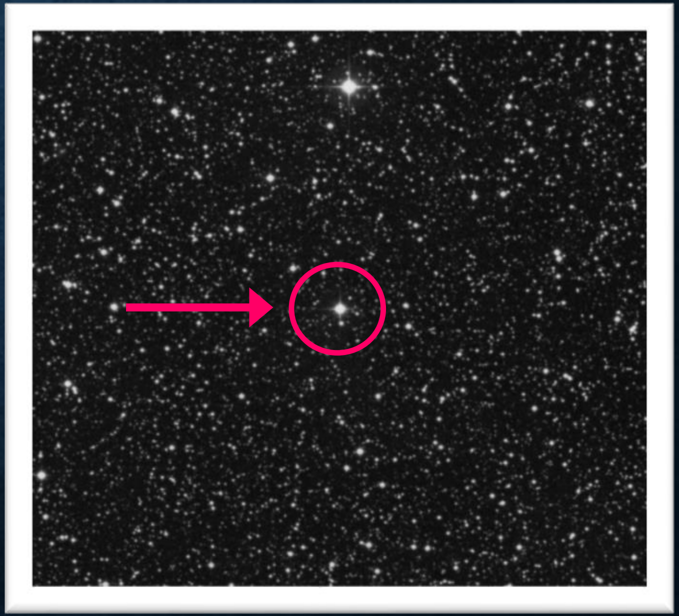

V1016 Cyg

# Introduction- Wind Accretion in Symbiotic stars

1. The mass losing giant shed material in the form of a slow stellar wind.
2. Some fraction of the slow stellar wind is accreted to the white dwarf.
3. Bipolar outflows may accompany the accretion disk around the white dwarf.
4. Bipolar nebular morphology appears common. Rodolfo Angeloni discovered a huge jet in Sanduleak's star.
5. Do we have a good observational tool to diagnose these activities?

→Yes, we do!!!

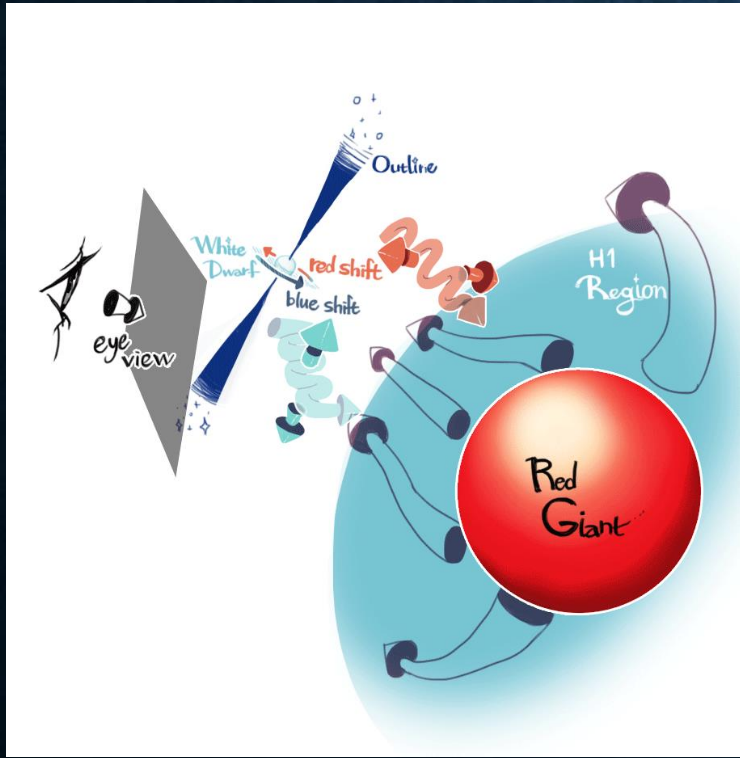


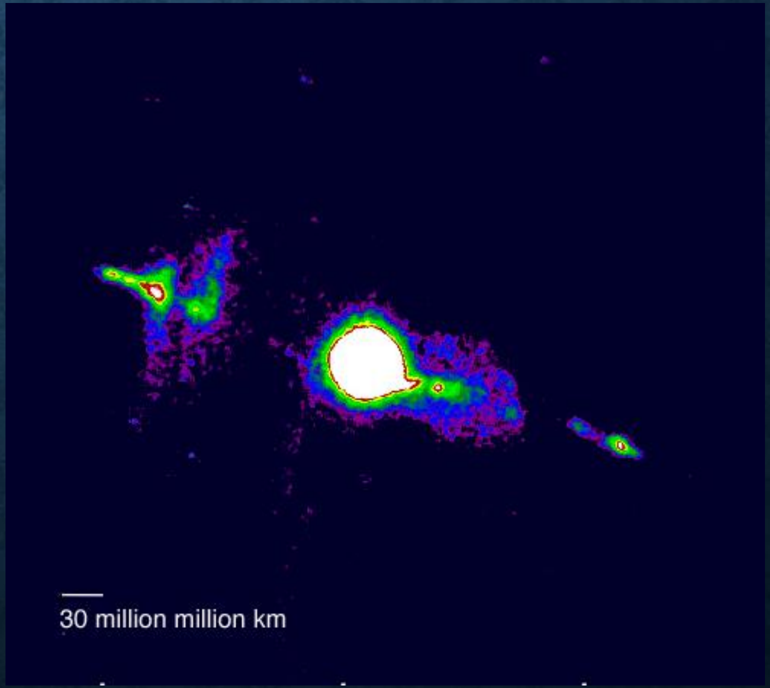


Sanduleak's star
(R. Angelnoni)

# Raman scattering in Symbiotic stars

1. Broad emission features at 6825 and 7082 with wavelength range of 20-30 Angstrom.
2. Schmid (1989) proposed that they are O VI 1032 and 1038 inelastically scattered by atomic hydrogen.
3. An invaluable spectroscopic and polarimetric tool to study the mass loss and mass transfer processes in symbiotic stars.

Astron. Astrophys. 211, L31–L34 (1989)

ASTRONOMY AND ASTROPHYSICS

*Letter to the Editor*

## Identification of the emission bands at λλ6830, 7088

H. M. Schmid

Institute of Astronomy, ETH Zentrum, CH-8092 Zürich, Switzerland

Received November 22, accepted December 20, 1988

**Summary.** Broad emission bands at 6830 Å and 7088 Å are observed in more than 50 per cent of symbiotic stars. Up to now these features have not been identified. They have only been observed in spectra of symbiotic binaries, which show high excitation emission and M–type absorption. I suggest that the emission features are due to Raman scattering of the OVI resonance doublet λλ1032, 1038 by neutral hydrogen. In this process the OVI photons are absorbed by hydrogen in its ground state $1s\,^2S$. The absorption leads to an intermediate state from where a photon is emitted, and the hydrogen atom is left in the excited state $2s\,^2S$. According to energy conservation the emitted photons have wavelengths of approximately 6830 Å and 7088 Å. Raman scattering can well explain the observed properties of the emission bands. Physical conditions required for efficient Raman scattering of OVI photons in symbiotic stars will be briefly discussed.

**Key words:** line identification – symbiotic stars – Raman scattering – emission spectra

### 1. Introduction

The spectra of symbiotic stars often show a strong, broad emission feature at λ6830. In a subset of stars a weaker but similar band can be observed at about λ7088. An example of these features is shown in Figure 1. The first detection of the λ6830 band was reported by Joy and Swings (1945). They observed that feature in the recurrent nova RS Oph during the 1933 outburst, where it was seen together with coronal emission lines. In later outbursts of RS Oph the λ6830 feature appeared again (e.g. Rosino and Iijima, 1987). Allen (1980) found that approximately half of the symbiotic stars exhibit the λ6830 band. In the same paper he extensively discusses possible identifications. He finds in particular that: (a) The λ6830 band is only observed in the spectra of symbiotic stars. It often ranks among the 10 most intense lines in the optical region, and may reach 5 per cent of the intensity of Hα. The λ7088 band is only seen in objects having strong λ6830 emission. The intensities of the two features correlate, they show an approximate ratio of $I(6830)/I(7088) \approx 4$. (b) The band profiles have a typical width of about 20 Å. The profiles vary strongly from star to star. In a given star there is a similarity between the λ6830 and λ7088 band profiles. (c) The λ6830 band is only observed in high excitation symbiotics showing [NeV] and [FeVII] lines. Thus the λ6830 emission seems to arise from an ion with an ionization potential above 100 eV.

In this letter the emission features λ6830 and λ7088 are identified as Raman scattering of the OVI resonance lines λλ1032, 1038 by neutral hydrogen. This process can explain all observational properties discussed in Allen (1980), and summarized above.

### 2. Raman scattering

A basic treatment of the theory for light scattering from a atom can be found in Loudon (1983). Raman scattering of OVI photons by hydrogen is possible, because there exists an excited hydrogen level with an excitation energy below the incident photon energy. Figure 2 shows schematically the scattering path of OVI λλ1032, 1038 on neutral hydrogen. The incident photon $\nu_i$ excites hydrogen from its ground state $1s\,^2S$ to an intermediate

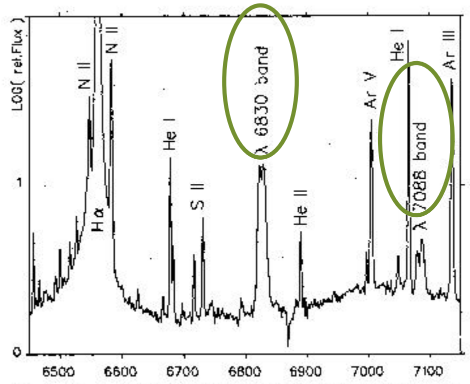


Fig. 1. Raman scattered emission bands in the symbiotic star V1016 Cyg. The spectrum was obtained on the 1.93m telescope at the Observatoire de Haute Provence.

# RAMAN SCATTERING OF O VI BY HI

1. A far UV photon is incident on a H I atom in the ground state.
2. During the interaction, the hydrogen atom is excited to one of infinitely many p states.
3. It can finally de-excite to either 1s state (Rayleigh scattering) or 2s state (Raman scattering)
4. The probability of scattering into 2s is about 1/6 smaller than that of scattering into 1s.

**Examples of Raman Scattering**

**Lyβ 1025 → Hα 6563**

**O VI 1032 → 6825**

**O VI 1038 → 7082**

$$h\nu_i = h\nu_o + h\nu_\alpha$$

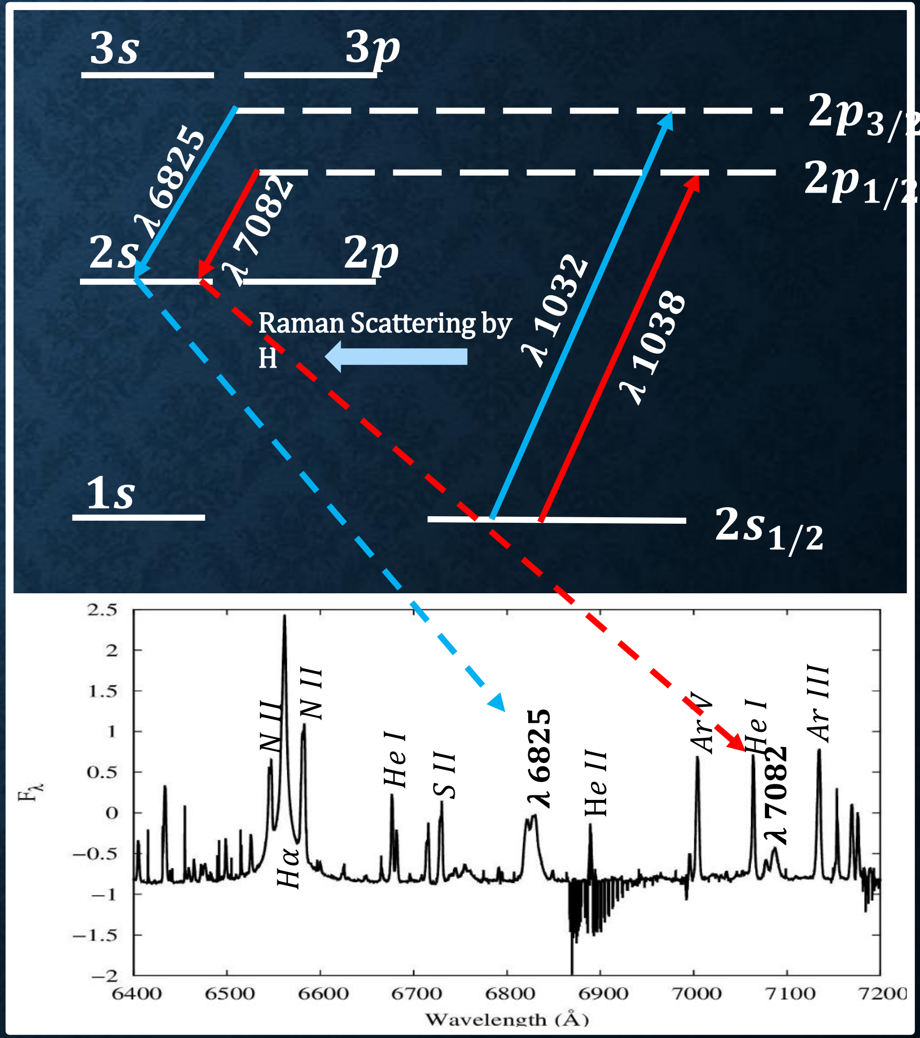

# SCATTERING CROSS SECTION (AROUND LYB)

2nd Order Time Dependent Perturbation Theory-
Kramers-Heisenberg Formula

Rayleigh Scattering

$$\left(\frac{d\sigma}{d\Omega}\right)_{Ray} = r_0^2 \left| \frac{1}{m\hbar} \sum_I \left( \frac{\omega (\boldsymbol{p} \cdot \boldsymbol{\varepsilon}^{\alpha'})_{AI} (\boldsymbol{p} \cdot \boldsymbol{\varepsilon}^{\alpha})_{IA}}{\omega_{IA}(\omega_{IA} - \omega)} - \frac{\omega (\boldsymbol{p} \cdot \boldsymbol{\varepsilon}^{\alpha})_{AI} (\boldsymbol{p} \cdot \boldsymbol{\varepsilon}^{\alpha'})_{IA}}{\omega_{IA}(\omega_{IA} + \omega)} \right) \right|^2$$

Raman Scattering

$$\left(\frac{d\sigma}{d\Omega}\right)_{Ram} = r_0^2 \left| \frac{1}{m\hbar} \sum_I \left( \frac{(\boldsymbol{p} \cdot \boldsymbol{\varepsilon}^{\alpha'})_{AI} (\boldsymbol{p} \cdot \boldsymbol{\varepsilon}^{\alpha})_{IA}}{\omega_{IA} - \omega'} - \frac{(\boldsymbol{p} \cdot \boldsymbol{\varepsilon}^{\alpha})_{AI} (\boldsymbol{p} \cdot \boldsymbol{\varepsilon}^{\alpha'})_{IA}}{\omega_{IA} + \omega'} \right) \right|^2$$

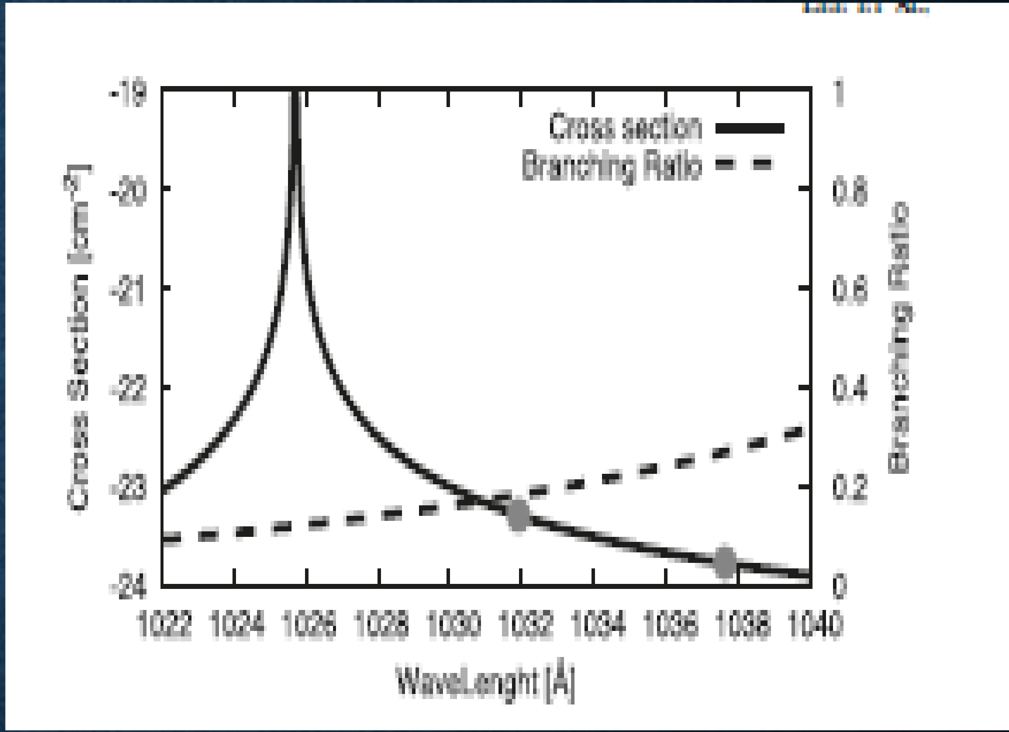


$$\boldsymbol{\sigma \approx 10^{-22} cm^2}$$ **for O VI**

Raman 6825 is stronger than 7082 by a factor of about 6.
Two factors are involved. One is the cross section, and the other is the flux ratio of resonance doublets.

1. Raman scattering operates in the presence of a thick neutral component in the vicinity of a strong far UV emission source.
2. HI is provided by the Giant and OVI by the white dwarf.

# MONTE CARLO SIMULATION OF RAMAN SCATTERING (Y.-M. LEE)

- Roughly one out of 5 scatterings of OVI 1032 with a hydrogen atom results in an emission of Raman OVI 6825 photon.
- Roughly one out of 3 scatterings for OVI 1038 into 7082.

(Significant difference in branching ratio as well as cross section)

- HI region is optically thick with respect to far UV but transparent to optical radiation.
- An O VI line photon keeps its identity as a far UV photon as long as it Rayleigh scatters with a hydrogen atom.
- An O VI line photon executes approximately 6 random walk steps before it takes a new identity as an optical photon redward of H alpha.
- An optical photon leaves the HI region without further interaction to reach us.

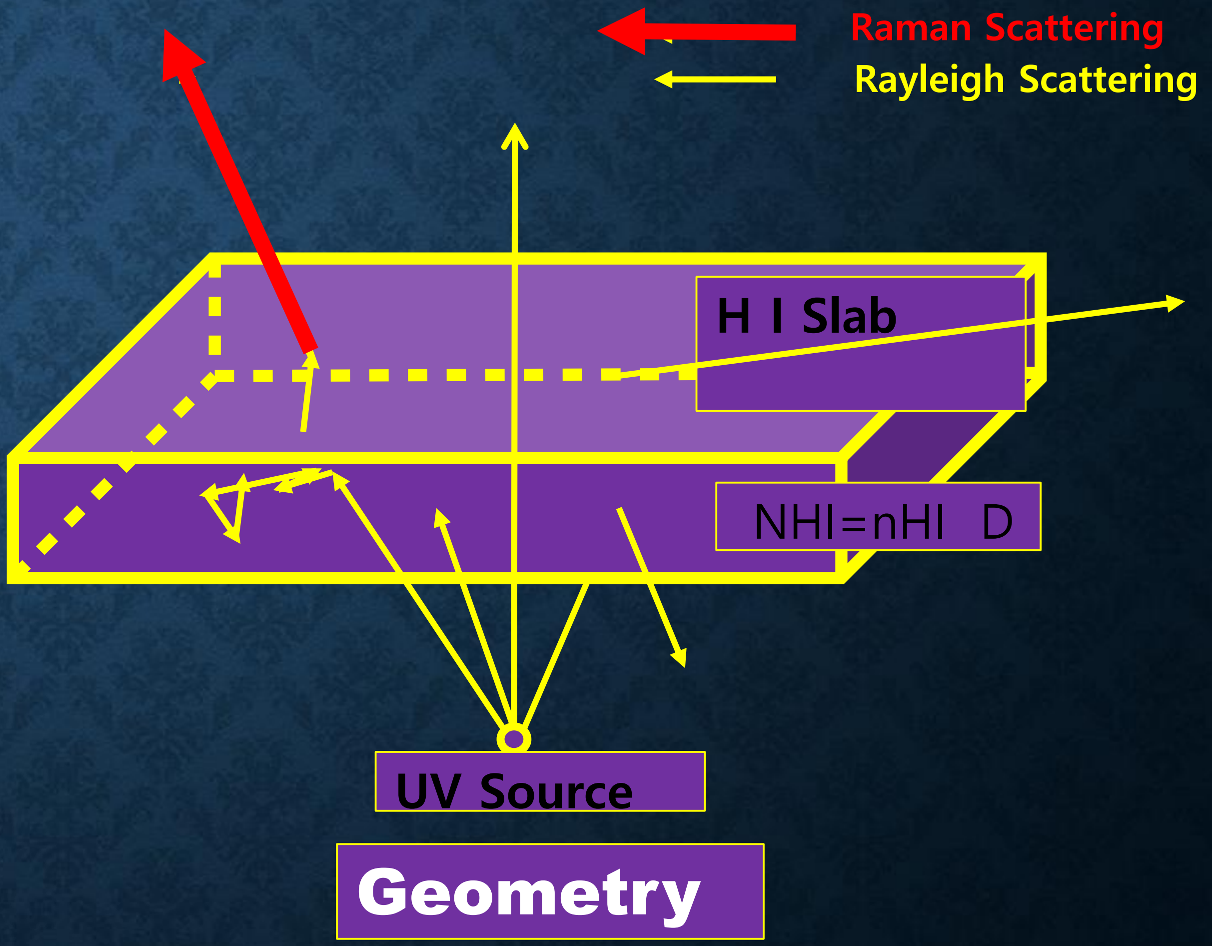

# Set the Geometrical Parameters

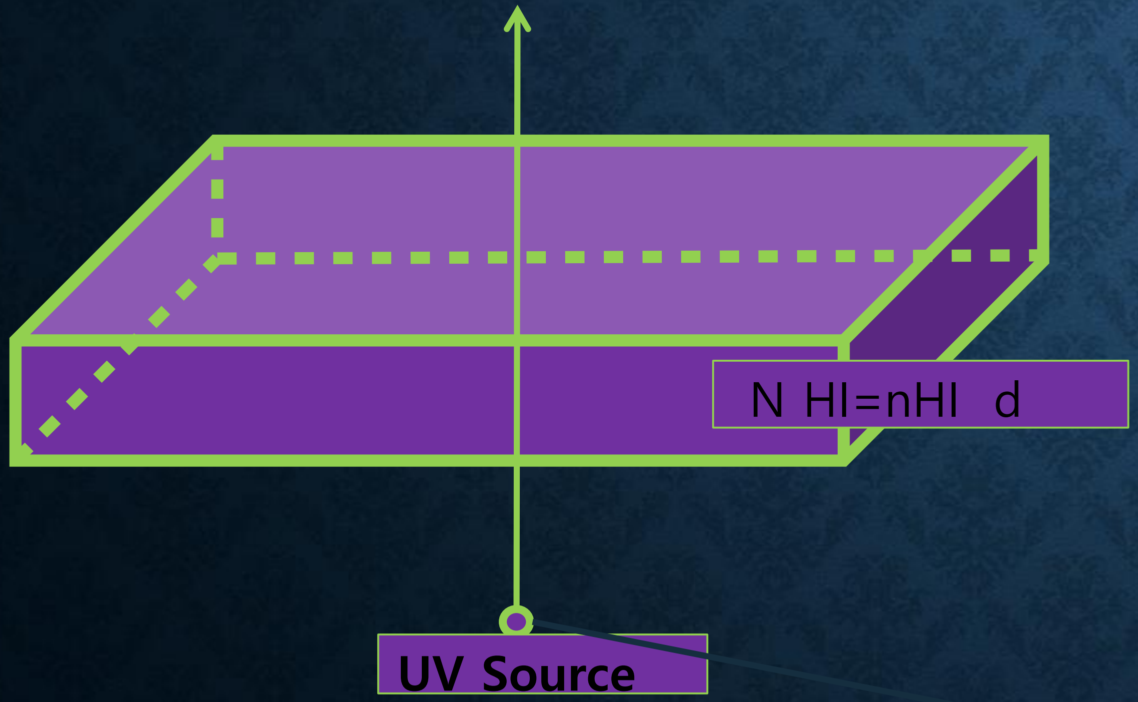


$$N_{HI} = n_{HI} d$$

$N_{HI}$ : **Column density (cm$^{-2}$)**

$n_{HI}$ : **Number density (cm$^{-3}$)**

$d$ : **Physical distance (cm)**

$\lambda_{max}, \lambda_{min}$ : **Maximum and minimum wavelength**

$f_{\lambda}$ : **The number of input photons**

# Monte Carlo Appoach of Radiative Transfer

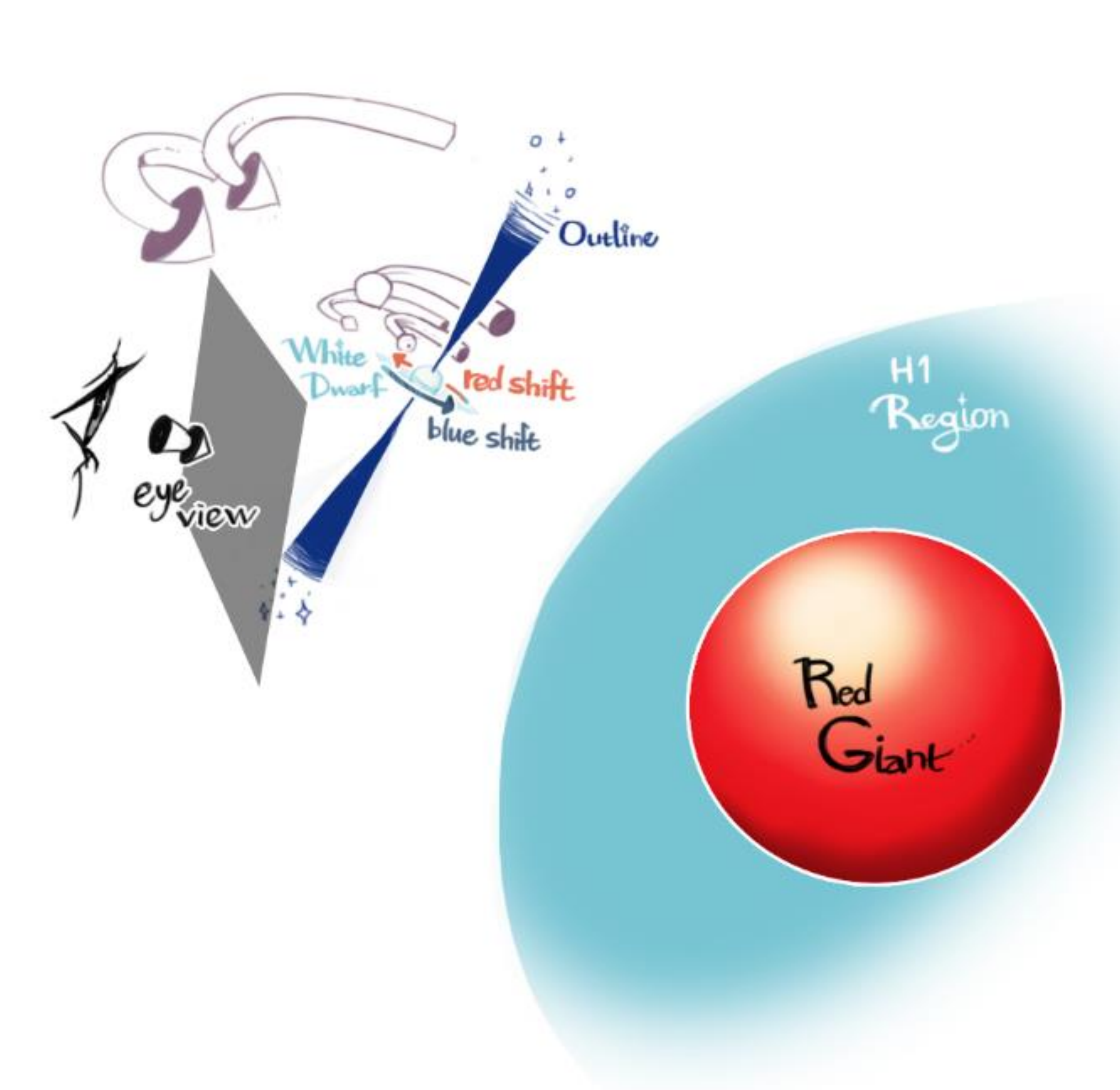


What fraction of OVI 1032 photons will be converted to Raman OVI at 6825? And what about OVI 1038 into Raman OVI 7082?

- The answer depends on the scattering geomtetry and content of HI.
- If the OVI source is fully embedded and there is sufficient amount of HI, then full Raman conversion is expected.
- If there is only small amount of HI atoms, single scattering processes dominate.

# FLUX RATIOS AND COLUMN DENSITY

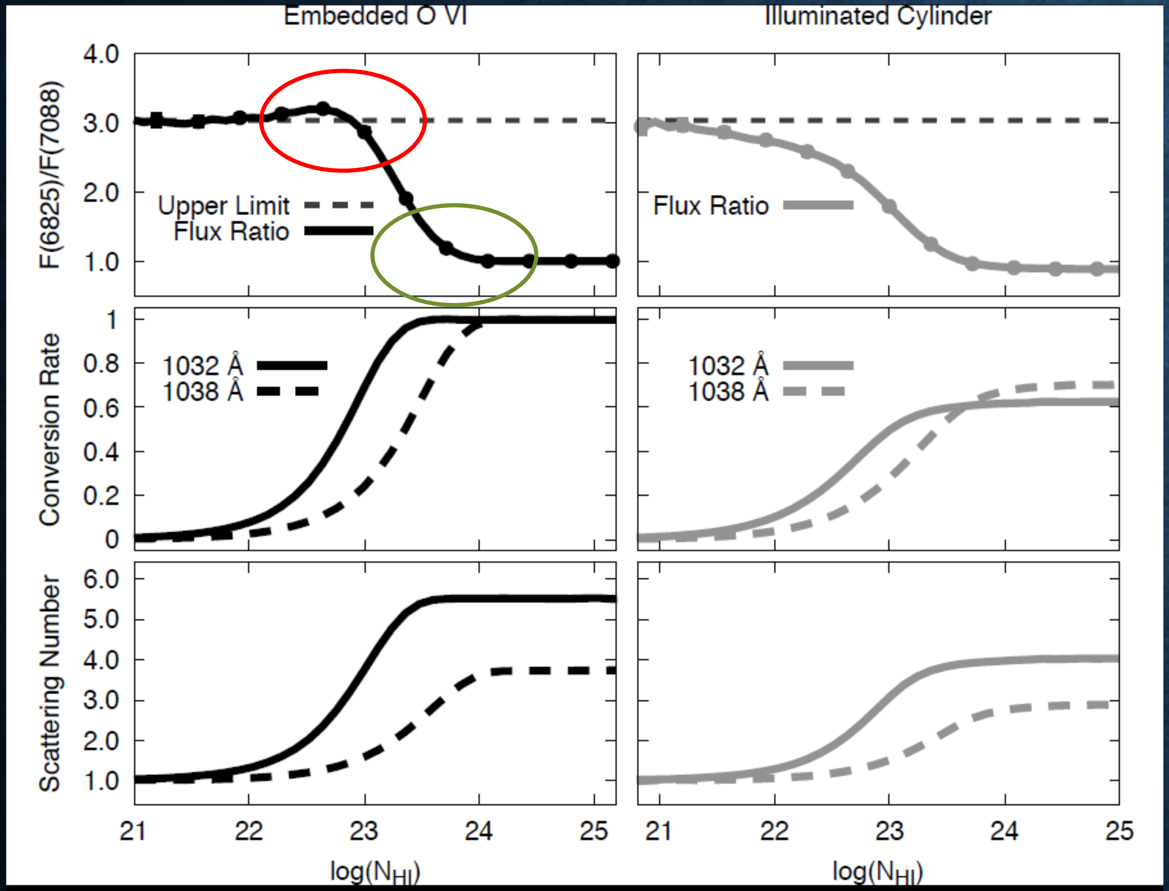


- Therefore as N_HI goes to infinity, Raman flux ratio of 6825 and 7082 approaches unity assuming that F1032/F1038 = 1.
- In the opposite limt of N_HI goes to 0, Raman conversion rate will be just the probability that a scattering takes place. (Perfect single scattering approximation). This is the product of total cross section times the branching ratio. OVI 1032 has three times higher probability of being converted to an optical photon than OVI 1038.

# CFHT OBSERVATIONS OF HM SGE AND AG DRA

S type symbiotics exhibit larger flux ratios of F6825/F7082 than D type symbiotic stars.

In S type symbiotics, the binary separation is smaller than in D type symbiotics. The HI region is much thicker in S symbiotics than in D symbiotics.

D type HM Sge

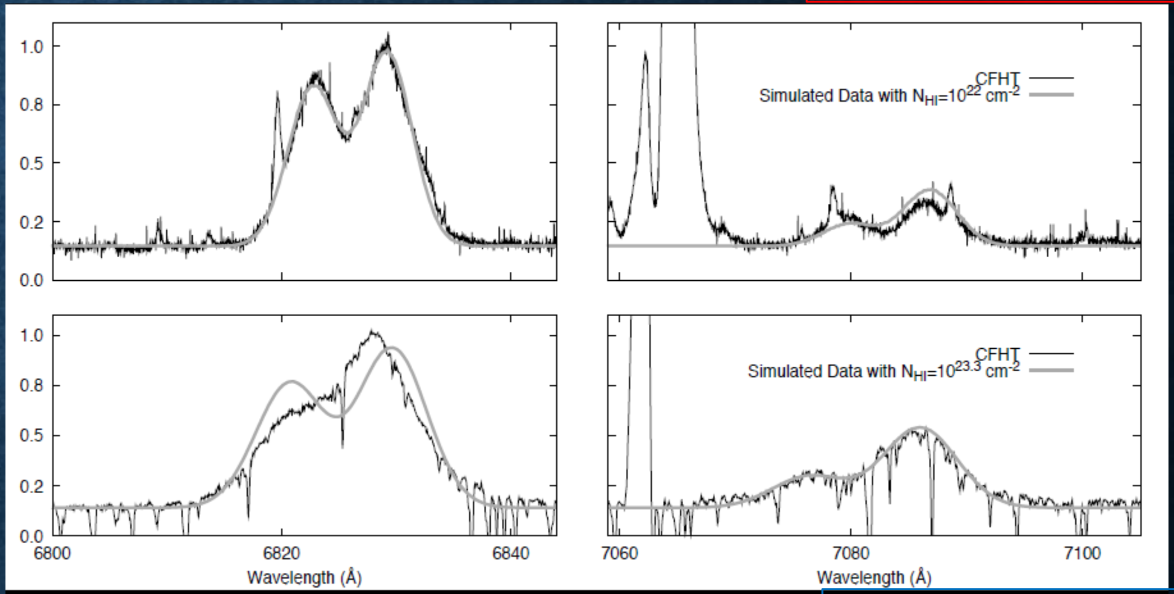


S type AG Dra

Y.-M. Lee et al. (2017)

# FURTHER EXAMPLES OF RAMAN SCATTERING (S.-J. CHANG)

- He II emits many far UV lines.
- 2n (n>1) → 2 transitions of He II mimics HI Lyman transitions. (Bohr atom or single-electron atom)
- He II 4→2 transition results in 1216, slighltly blueward of HI Ly alpha 1216.
- He II 6→2 gives 1025 and Raman scattered to form 6545 feature. → Sekeras & Skopal (2015)
- Highly useful to put constraints on the mass loss rate of the giant component in symbiotic stars.

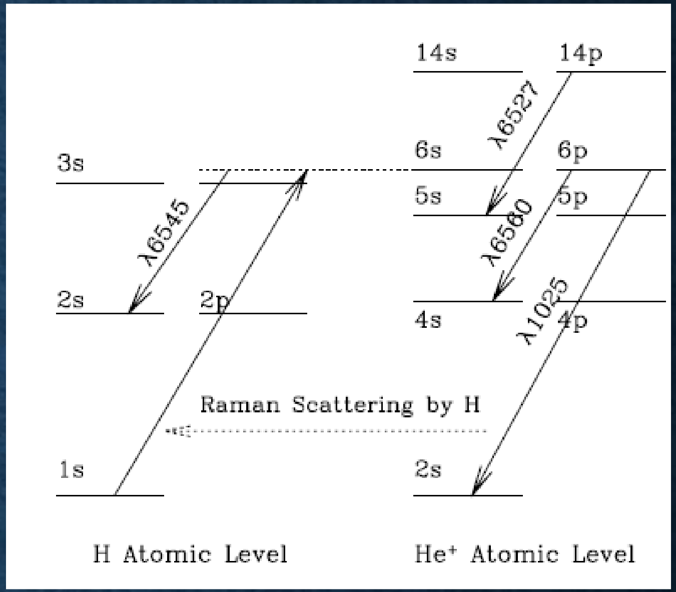


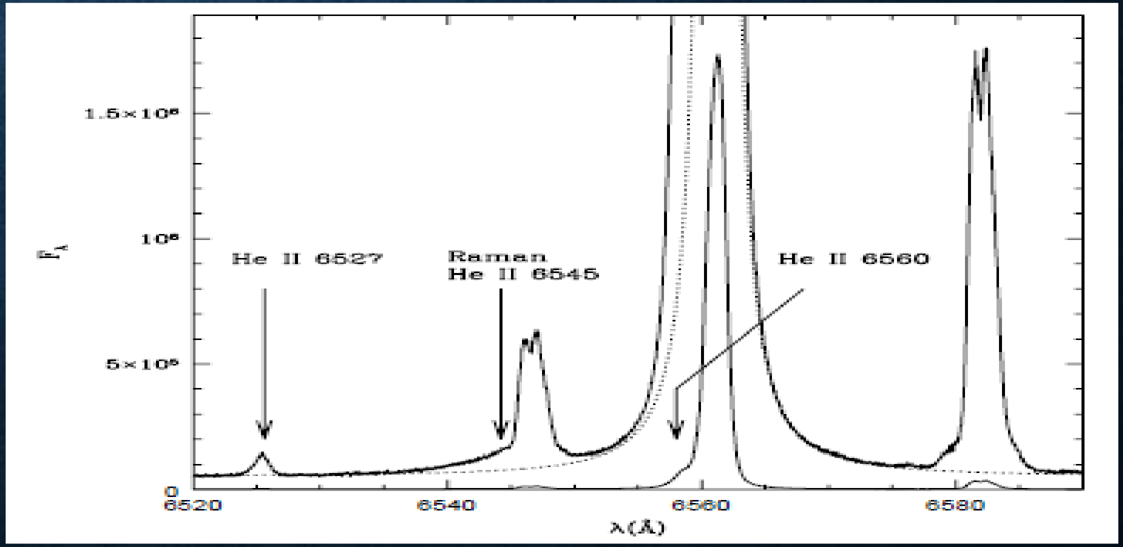

# IONIZATION STRUCTURE

Taylor and Seaquist 1984

X is a photoionization parameter that relates the mass loss rate and ionizing luminosity.

$$X = \frac{4\pi\mu^2 m_p^2}{\alpha} a L_{ph} (v_\infty / \dot{M})^2$$

$$\mathbf{v}_H(\mathbf{r}) = v_\infty (1 - R_*/r)^\beta \hat{\mathbf{r}},$$

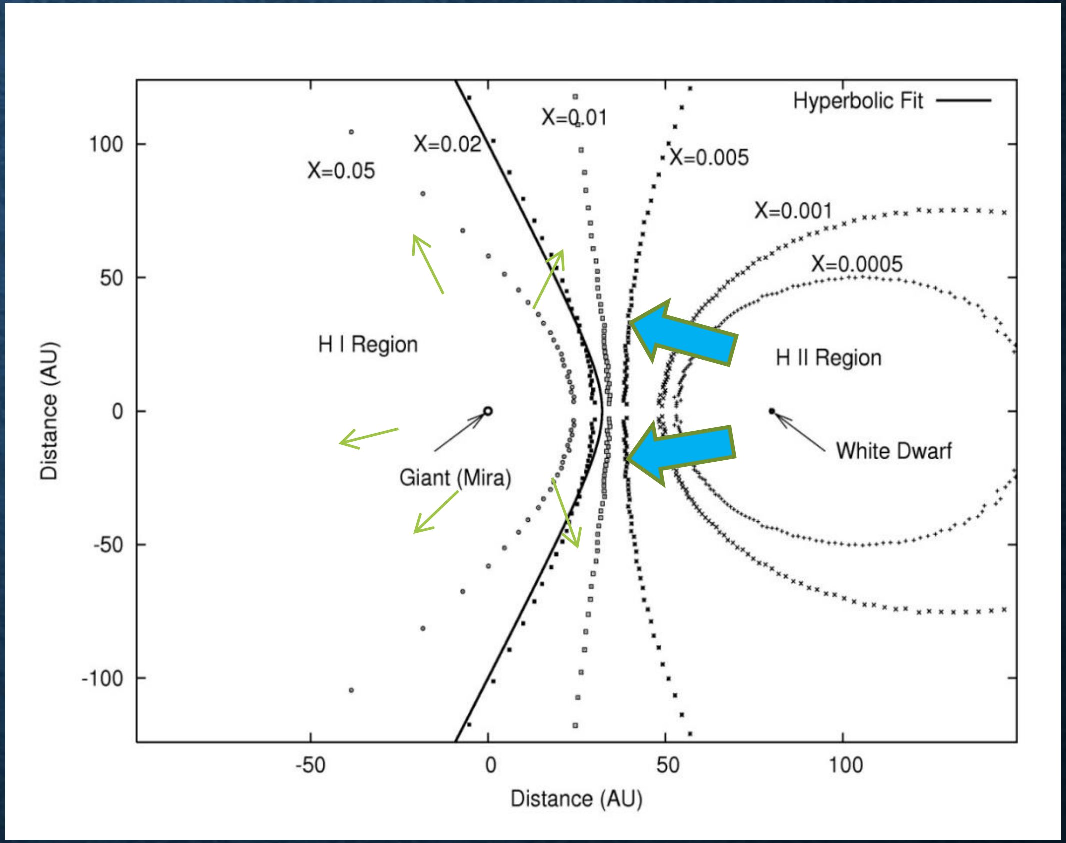

# RAMAN SCATTERING OF HE II

- Seok-Jun Chang is comparing the Raman conversion efficiencies of He II10→ 2 (949), He II 8→2 (972) and He II 6→2 (1025) in their formation of Raman features at 6545, 4850 and 4330 blueward of H alpha, H beta and H gamma.

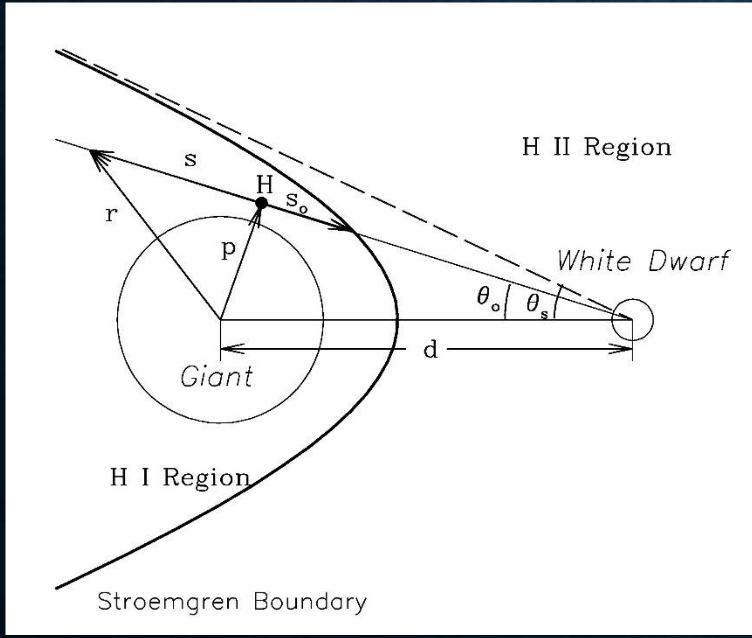


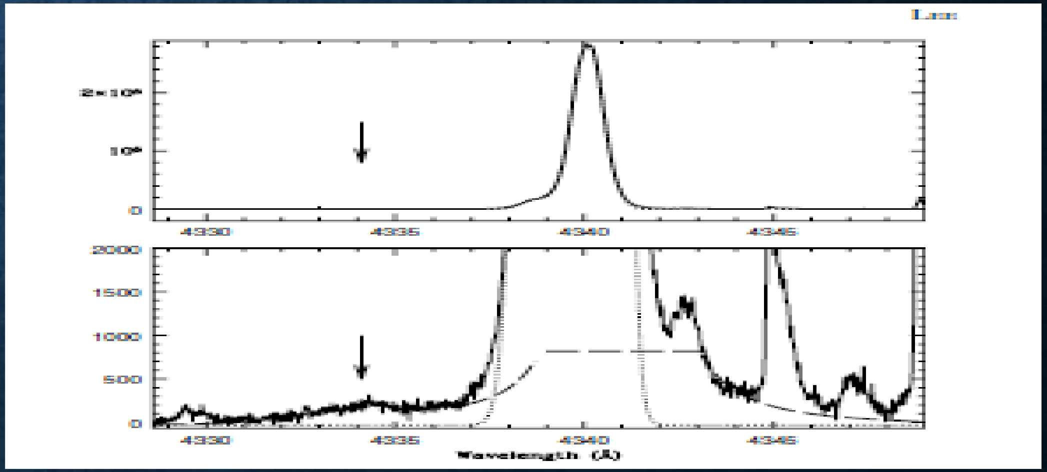


Raman 4332 feature in V1016 Cyg (Lee 2012)

# PROFILE FORMATION OF RAMAN OVI IN SYMBIOTICS (J.-E. HEO)

- O VI emission region may be mainly identified with the accretion flow around the white dwarf.
- The accretion flow tends to be convergent on the entrance side whereas it is divergent on the opposite side.
- More O VI photons are generated on the convergent side than on the opposite side, resulting in red-enhance Raman profiles.

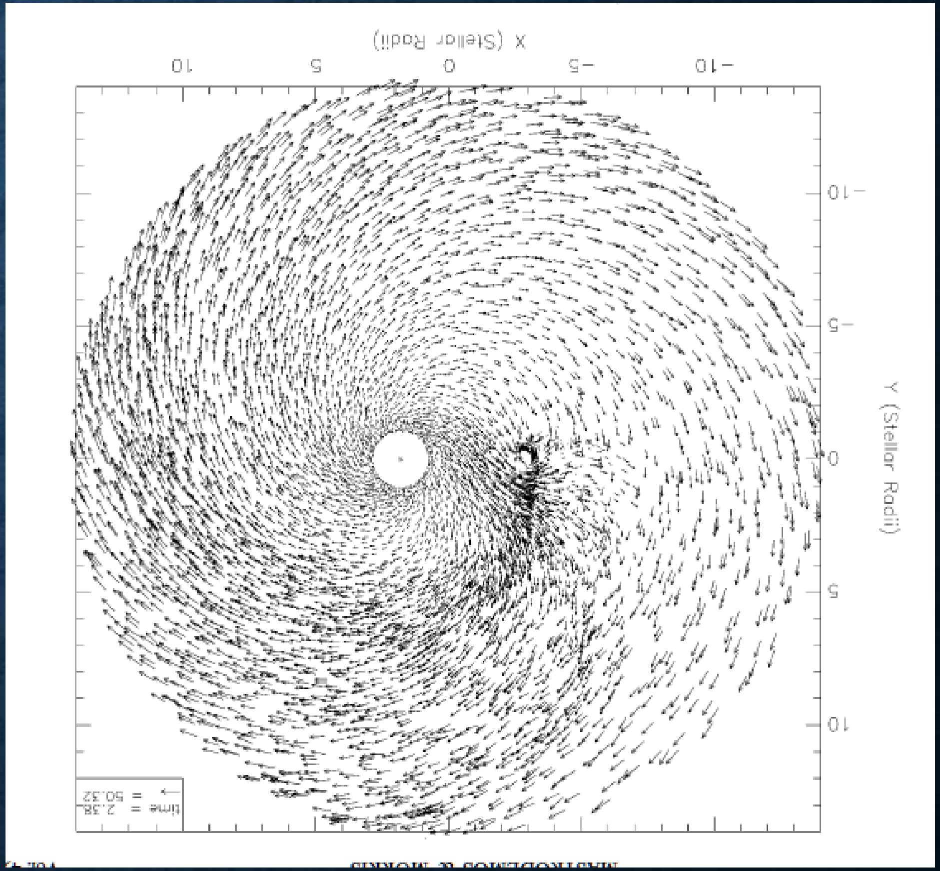


SPH simulation by Mastrodemos and Morris (1998)

Raman OVI profiles harbor intricate information about accretion flow around the white dwarf.

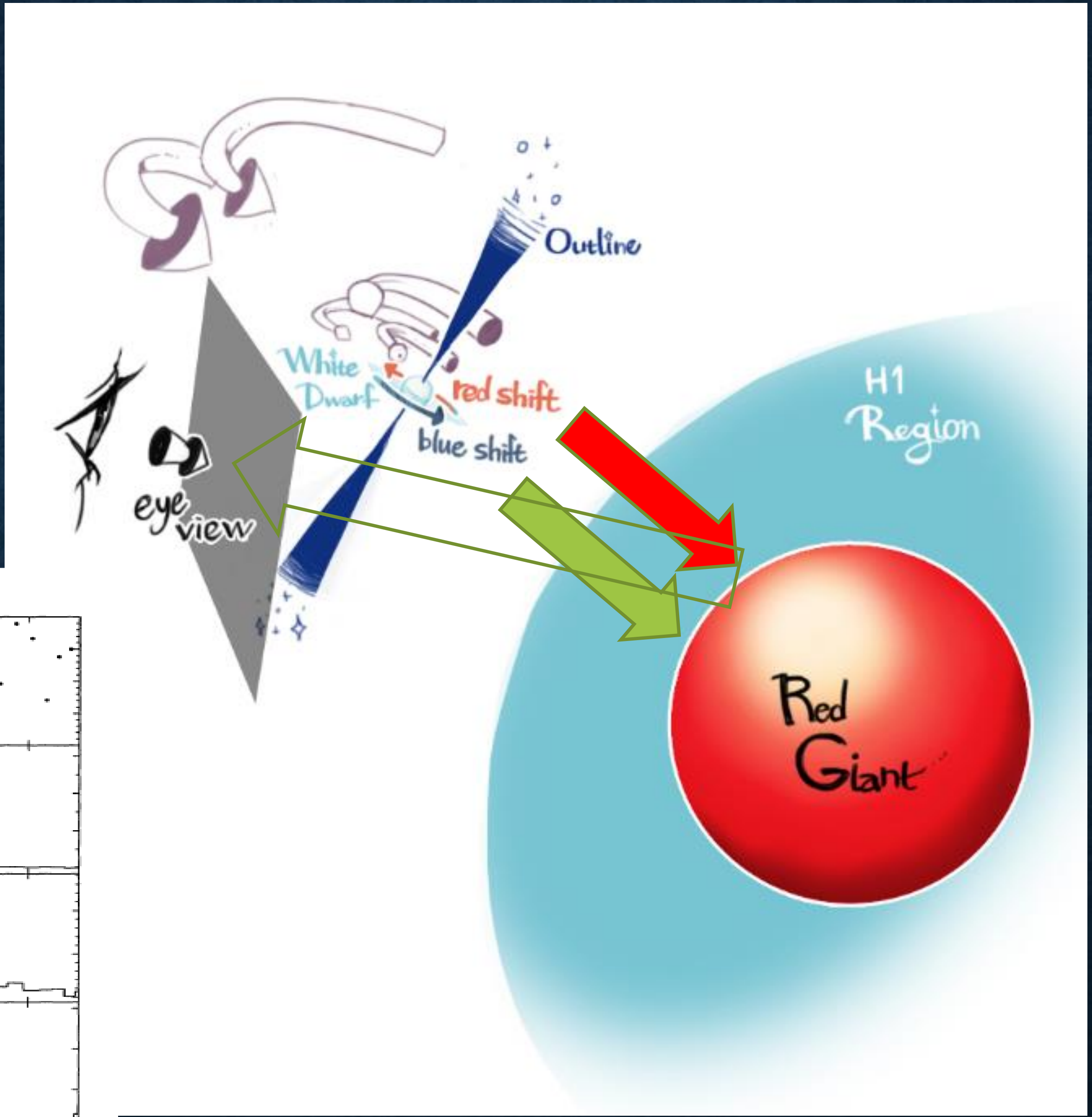


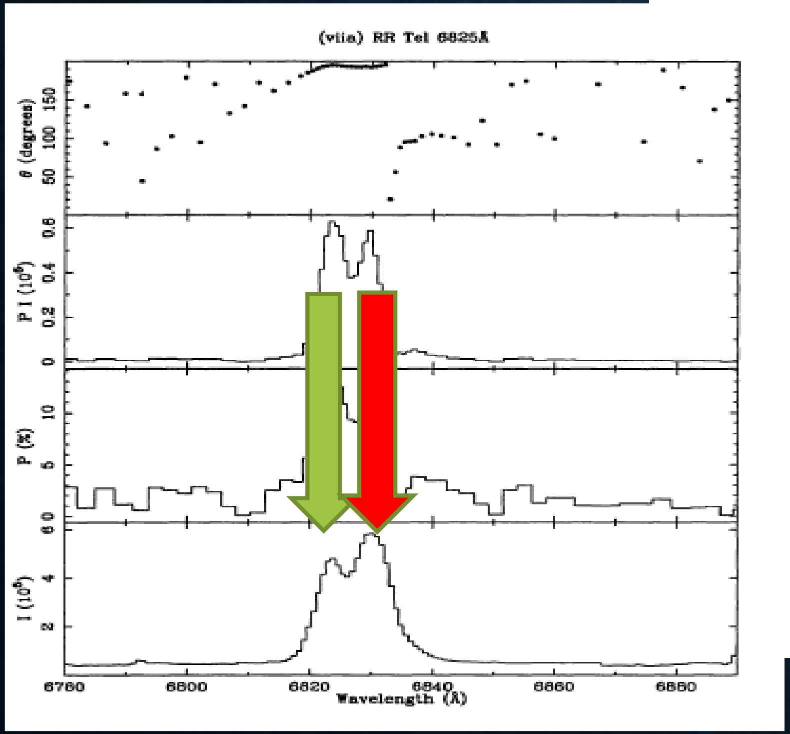

# PROFILE BROADENING OF RAMAN SCATTERED FEATURES

- $h\nu_i = h\nu_o + h\nu_\alpha \rightarrow \nu_i = \nu_o + \nu_\alpha$
- $\Delta\nu_i = \Delta\nu_o$
- $\frac{\Delta\nu_i}{\nu_i} = \frac{\Delta\nu_o}{\nu_i} = \frac{\nu_o}{\nu_i}\frac{\Delta\nu_o}{\nu_o}$

Far UV OVI 1032

- This relation implies that the Raman scattered features will be broadened by the factor $\lambda_o/\lambda_i$
- In the case of Raman 6825, this factor is almost 6, resulting in a very broad emission feature.
- The Raman profile reflects the relative kinematics between the neutral region and far UV emission region and is totally irrelevant to the observer's line of sight.
- Nature installed a wonderful **mirror** in front of the giant to provide an edge-on view of the accretion flow and a lateral view of the collimated outflow.
- (Jeong-Eun Heo's Work)

Raman OVI 6825

# PROFILE BROADENING – HOW CAN WE UNDERSTAND IT?

- Imagine an observer who is receding from an O VI emitter with a speed slightly less than speed of light.
- This observer measures the wavelength of OVI with a huge redshift z.
- For example if z=5, then the measured wavelength would be 1032 X (1+5) = 7192.
- For this observer, the O VI emitter appears to move very slowly by a factor of (1+z) because of cosmic time dilation.
- Raman scattering provides a similar wavelength stretch by a factor ~6. This is like we are observing an early universe of redshift z~5.
- Compared to the speed of light, if the internal motion of O VI emission region is negligible, then the observed wavelength is mostly independently of the observer's line of sight.

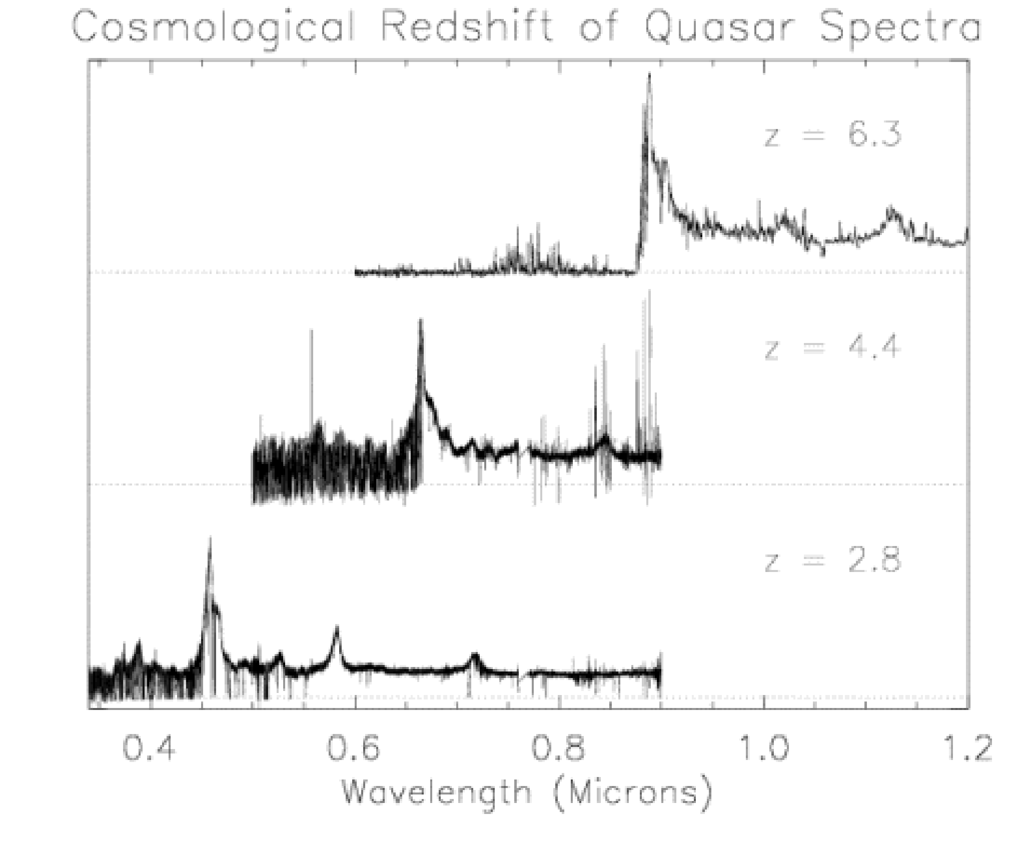

# UV SPECTRA OF SYMBIOTICS

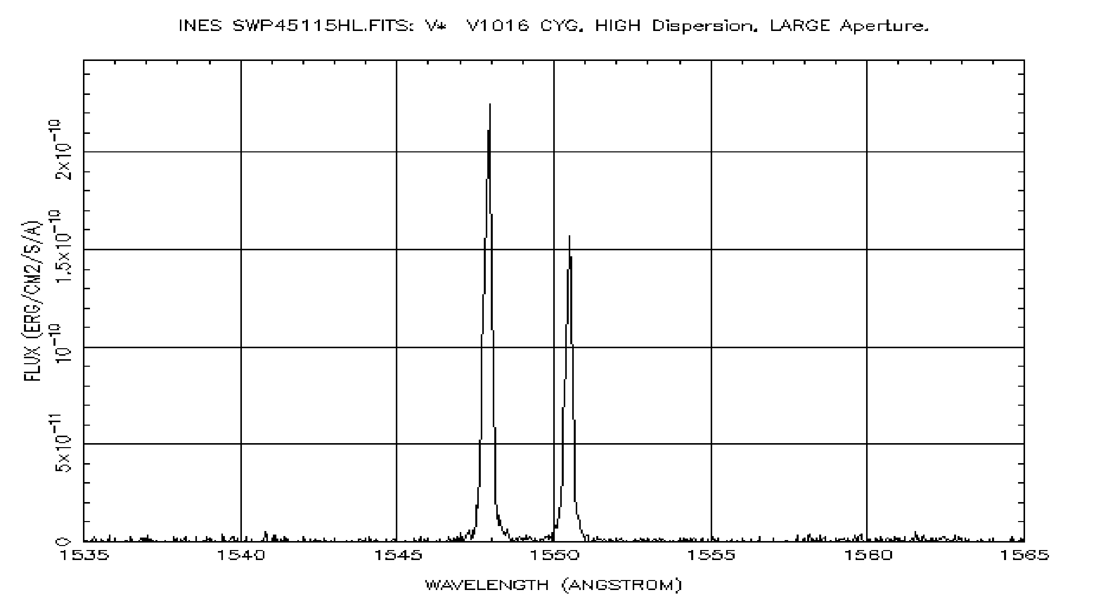


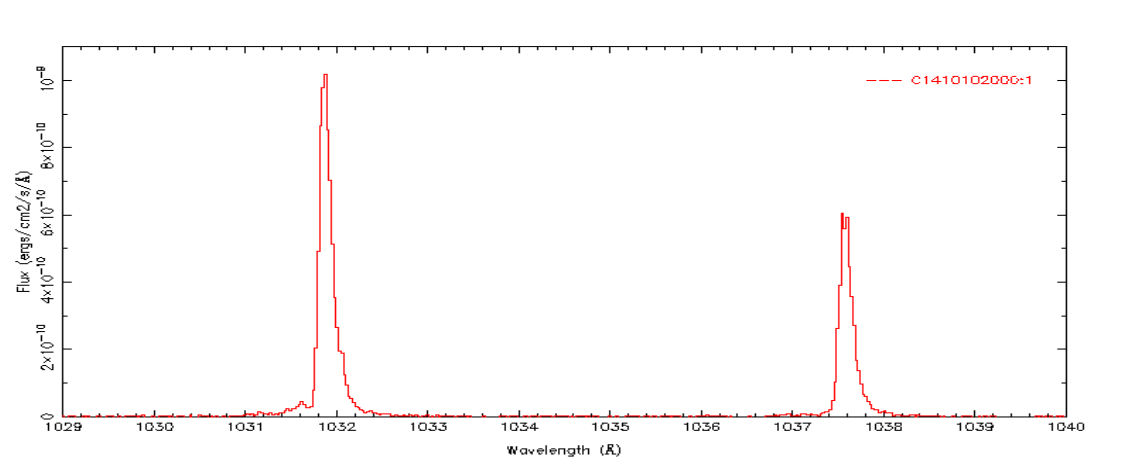


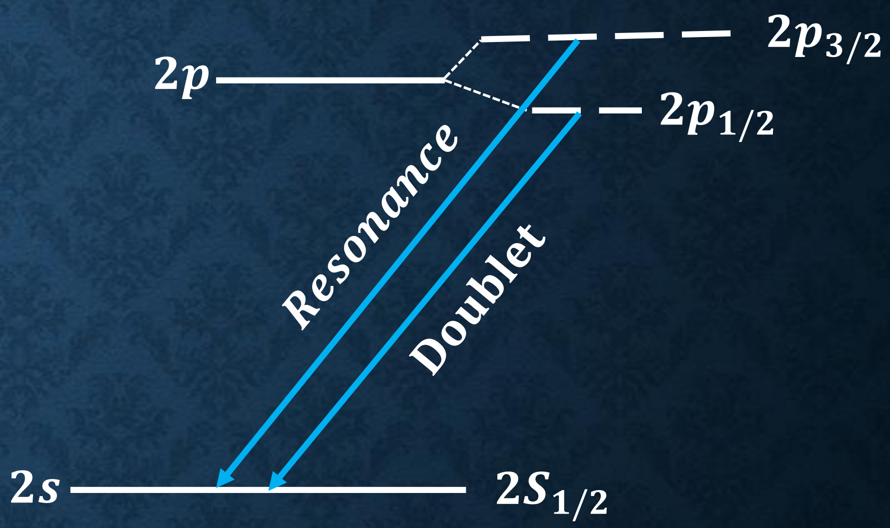


Resonance Doublet

Atomic structure of Li-like Ions

C IV 1548, 1551 Å

N V 1238, 1243 Å

O VI 1032, 1038 Å

In the optically thick medium, the doublet flux ratio approaches unity.

# Profile Analysis

- Adopting an accretion disk model, we may explain a double peak profile
- Accretion disk has a physical dimension of ~1 AU.
- The velocity scale is 30-50 km/s.

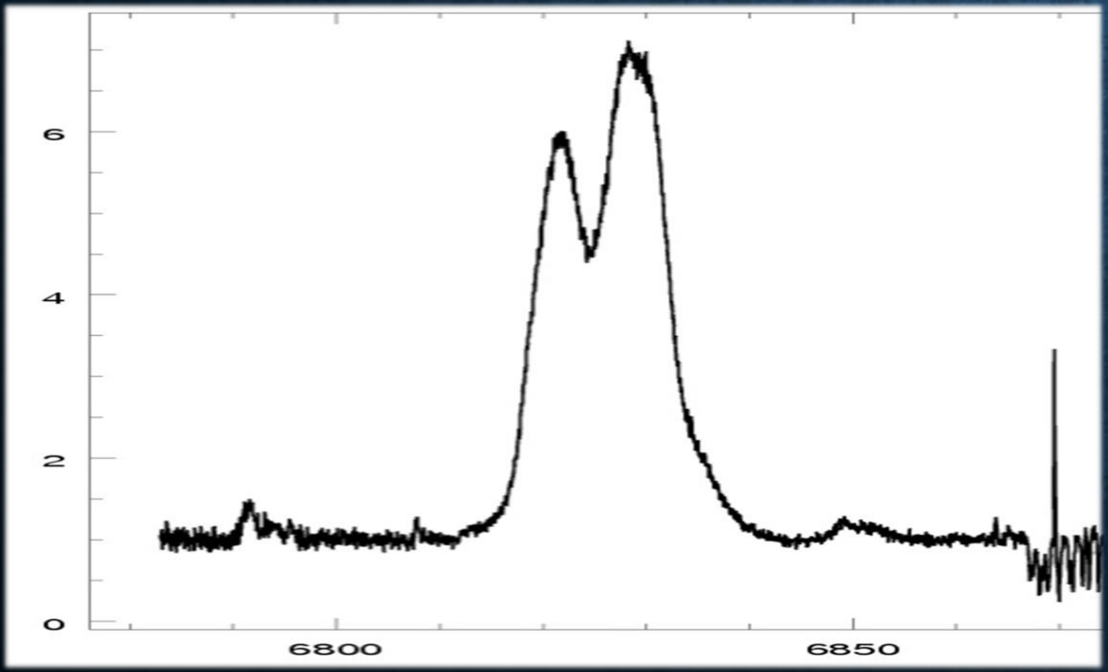


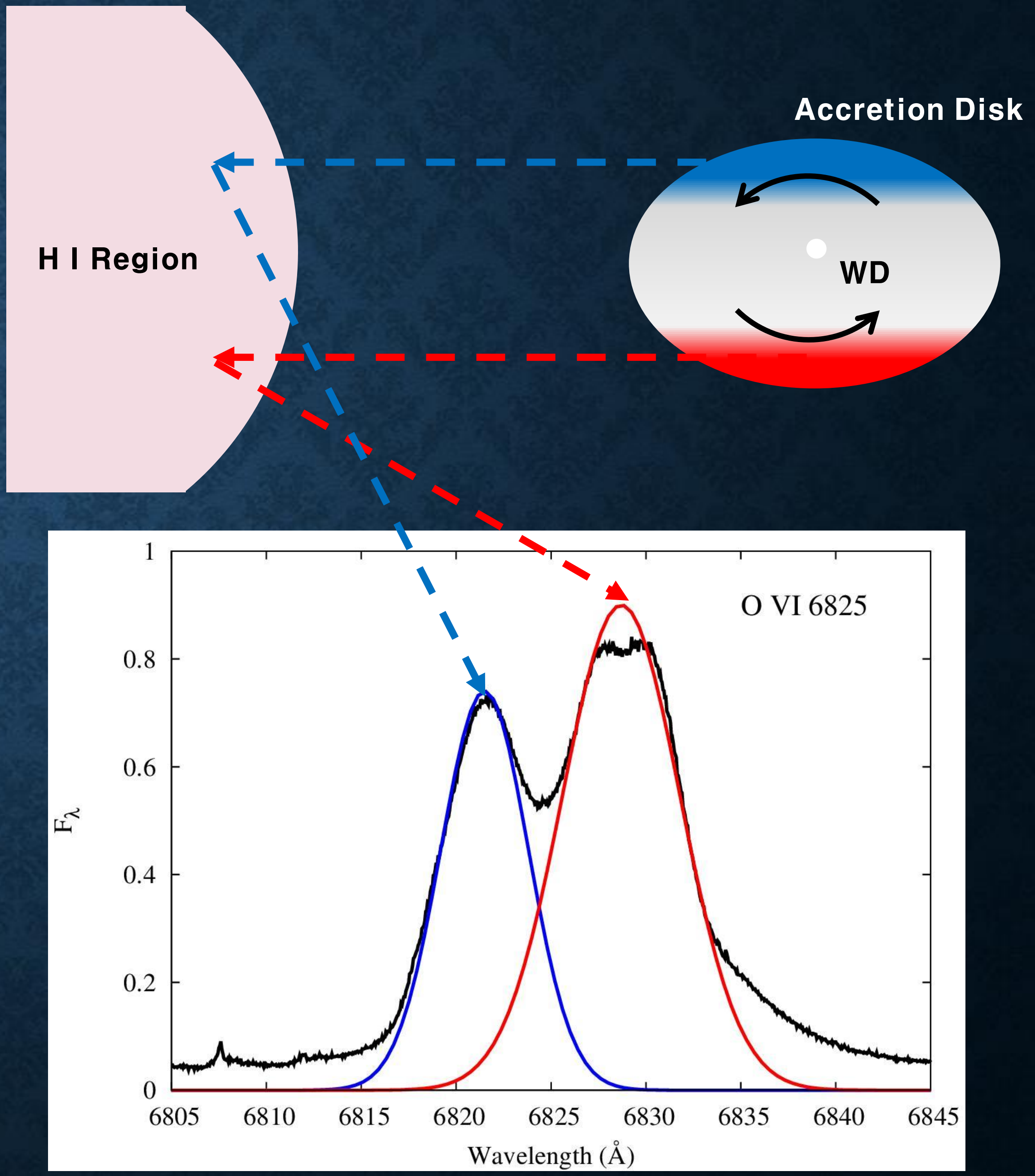

# PROFILE COMPARISONS OF 6825 AND 7082 (JEONG-EUN'S TALK)

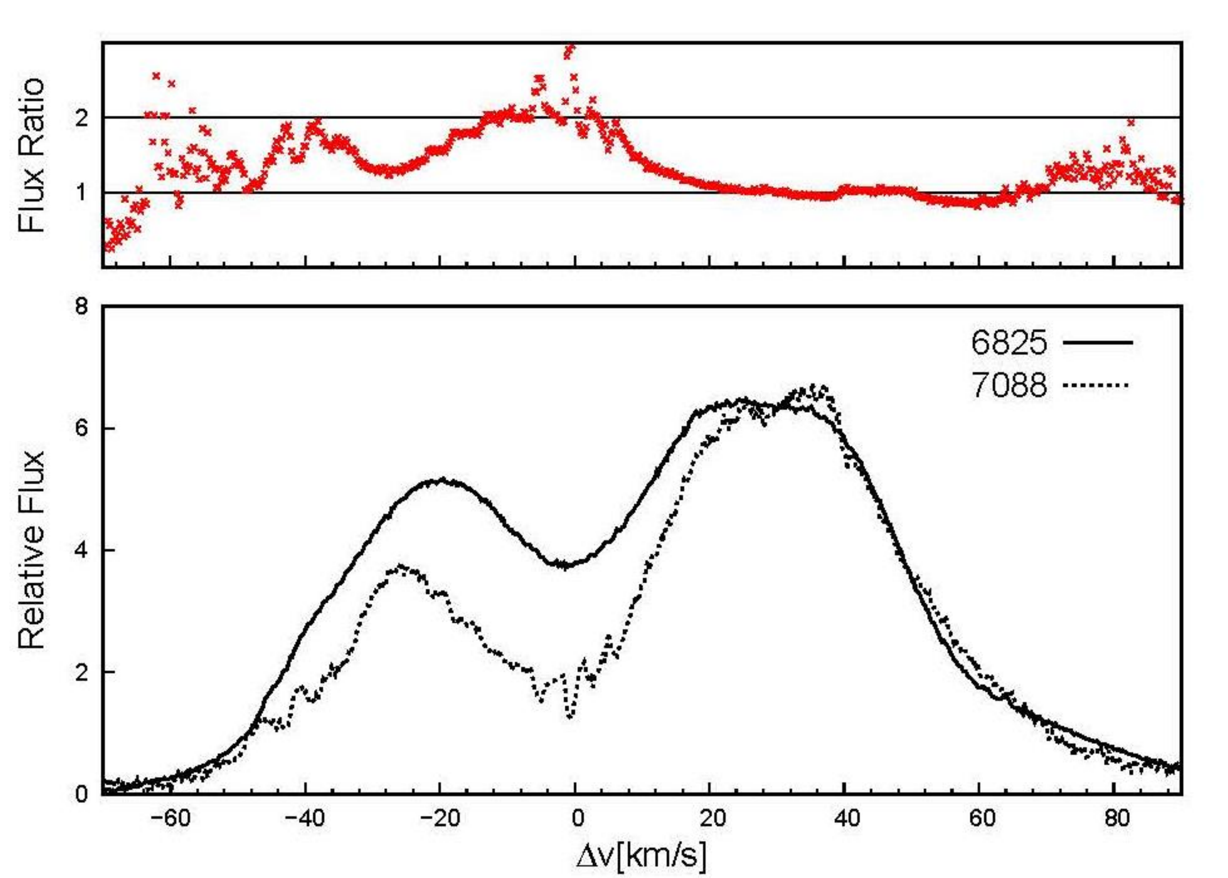


- Symbiotic Star V1016
- The flux ratio should be in the range of 1:1 and 2:1.
- We plot the two profiles in the Doppler factor space with the normalization of equal red peaks.
- Deficit of the blue part of the 7082 feature is conspicuous.
- What is this implying?

# Spectropolarimetry of the Symbiotic Nova RR Tel around 6825 and 7082

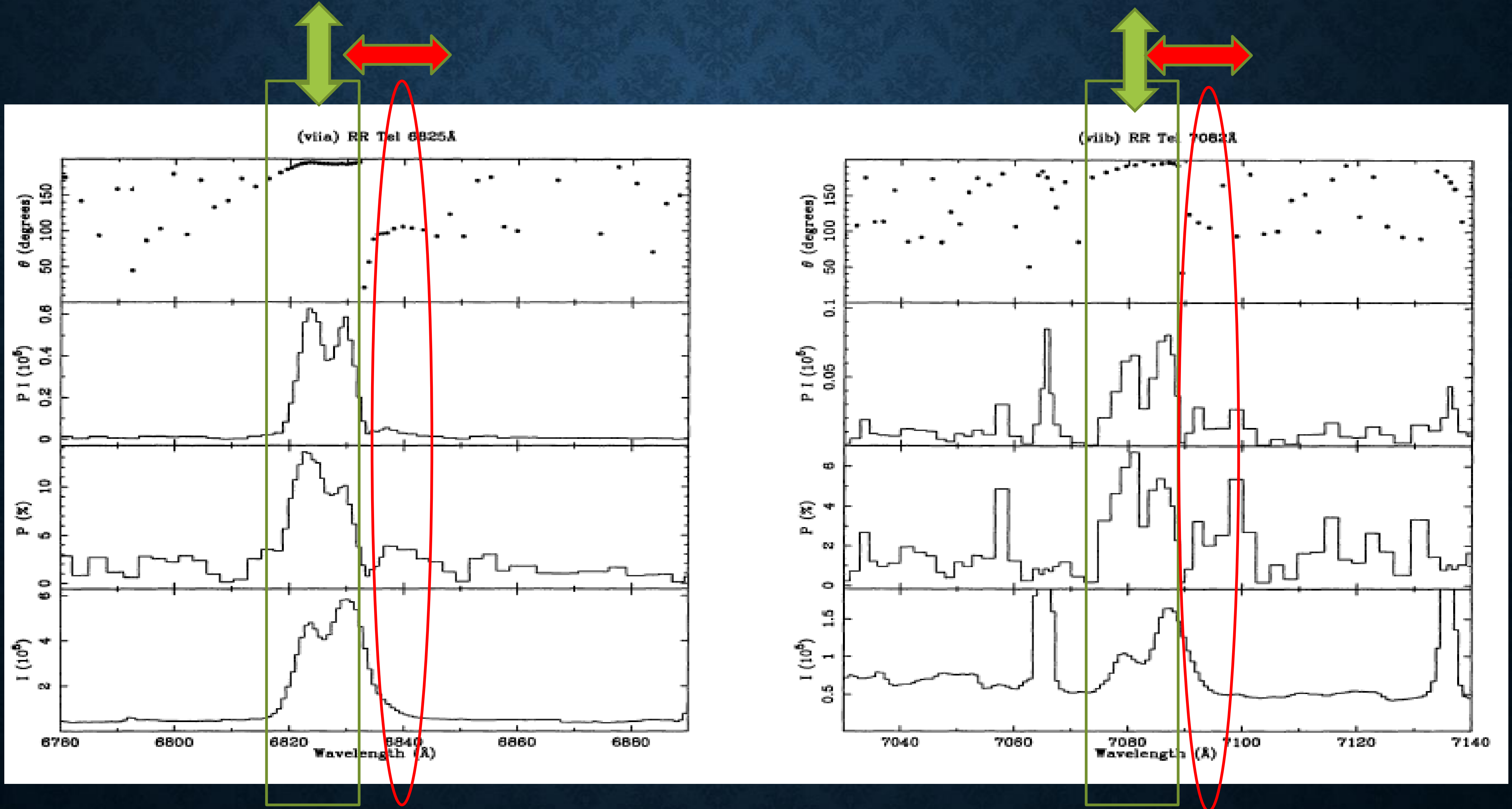

# Polarization of transveres waves

1. Transverse waves can be polarized in two directions perpendicular to the direction of propagation.
2. One can generate polarized waves by oscillating the source in the specific direction.
3. Natural light is usually unpolarized.
4. Artificial light like LCD or scattered light can be strongly polarized.

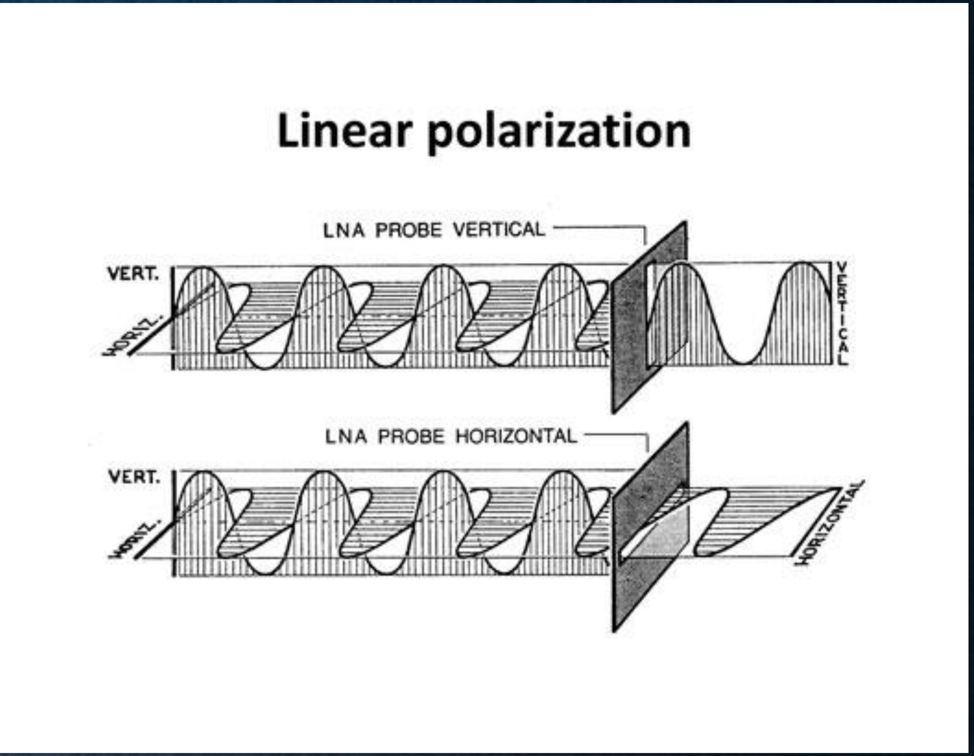


- If we watch an unpolarized light source, no brightness changes occurs when we rotate the polarization filter.
- For a polarized source, the brightness changes when we observe it using polarization filters.

# POLARIZED LCD LIGHT

1. NEMATIC MOLECULAR STRUCTURE!
2. HUMAN EYE DOESN'T DISCERN POLARIZED LIGHT FROM UNPOLARIZED LIGHT.
3. IMAGE CAN BE FORMED BY APPLYING A SMALL ELECTRIC FIELD TO SPECIFIC PIXELS THAT DELINEATE THE IMAGE.

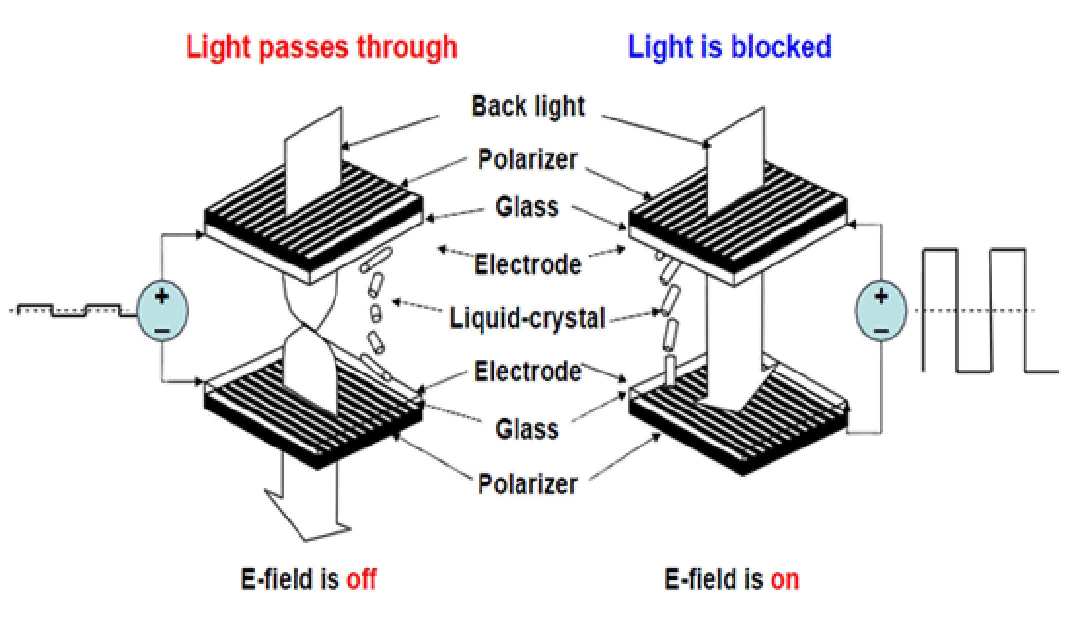


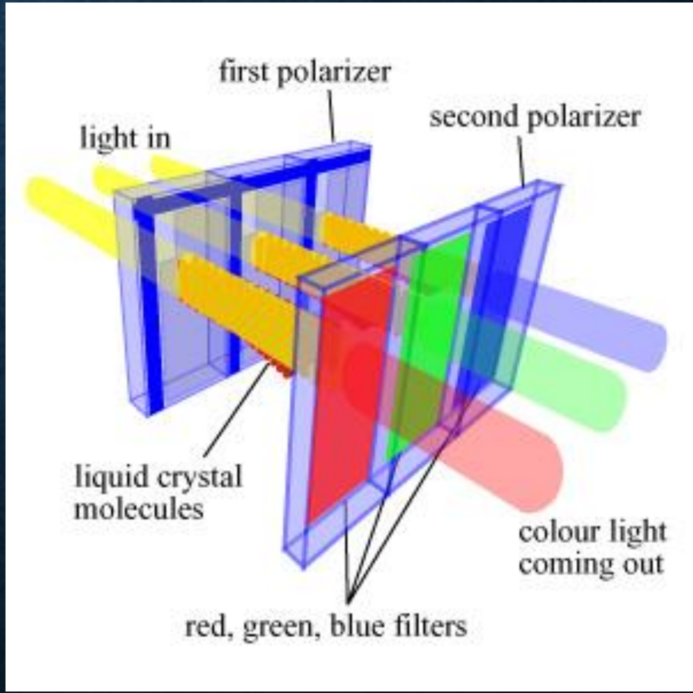

# Polarization of scattered radiation

1. Scattered light is usually significantly polarized.
2. A unique plane can be chosen if we are given two vectors. In a scattering event, the scattering plane is naturally defined by the wavevectors for incident and outgoing radiation.
3. Because of the transverse nature, oscillation in the direction perpendicular to the scattering plane is favored.

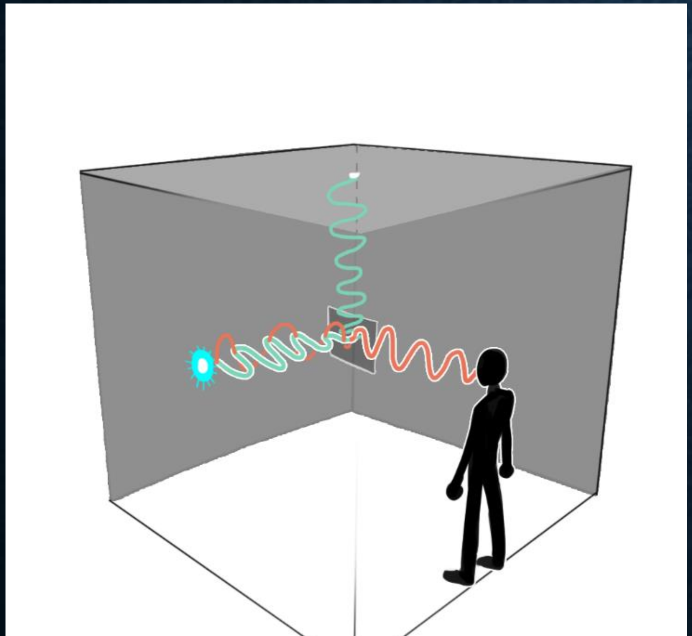

The red wing part is perpendicularly polarized with respect to the main double peak part!!!

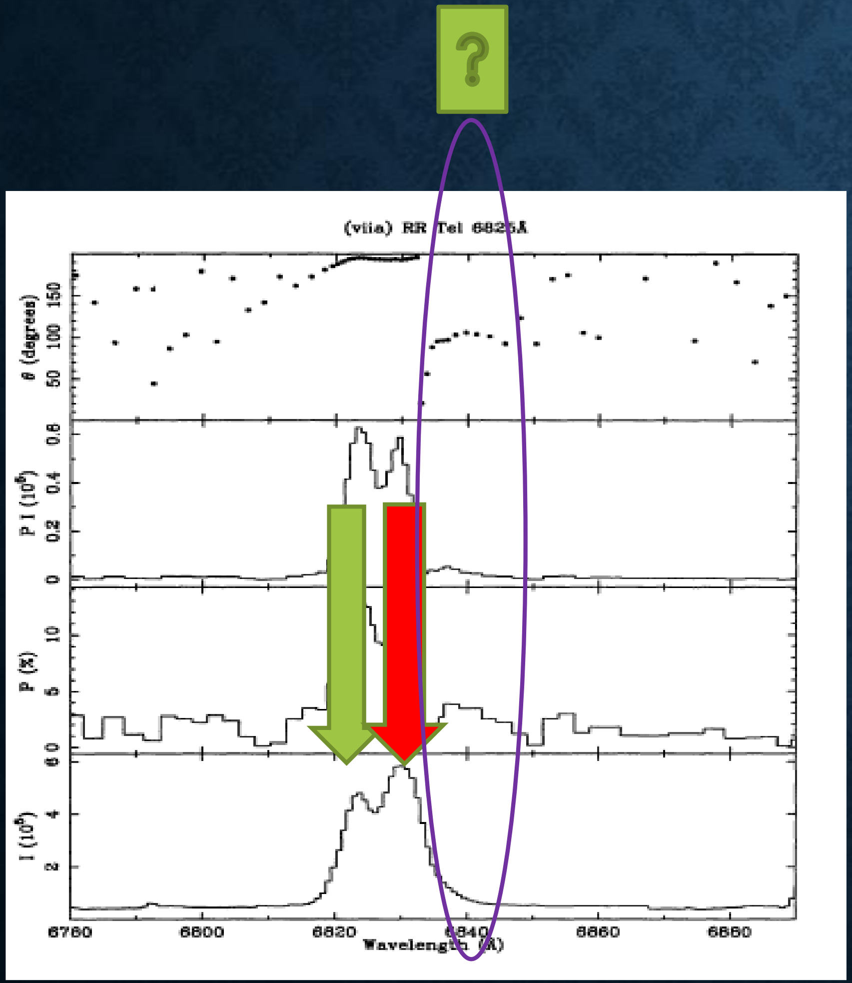


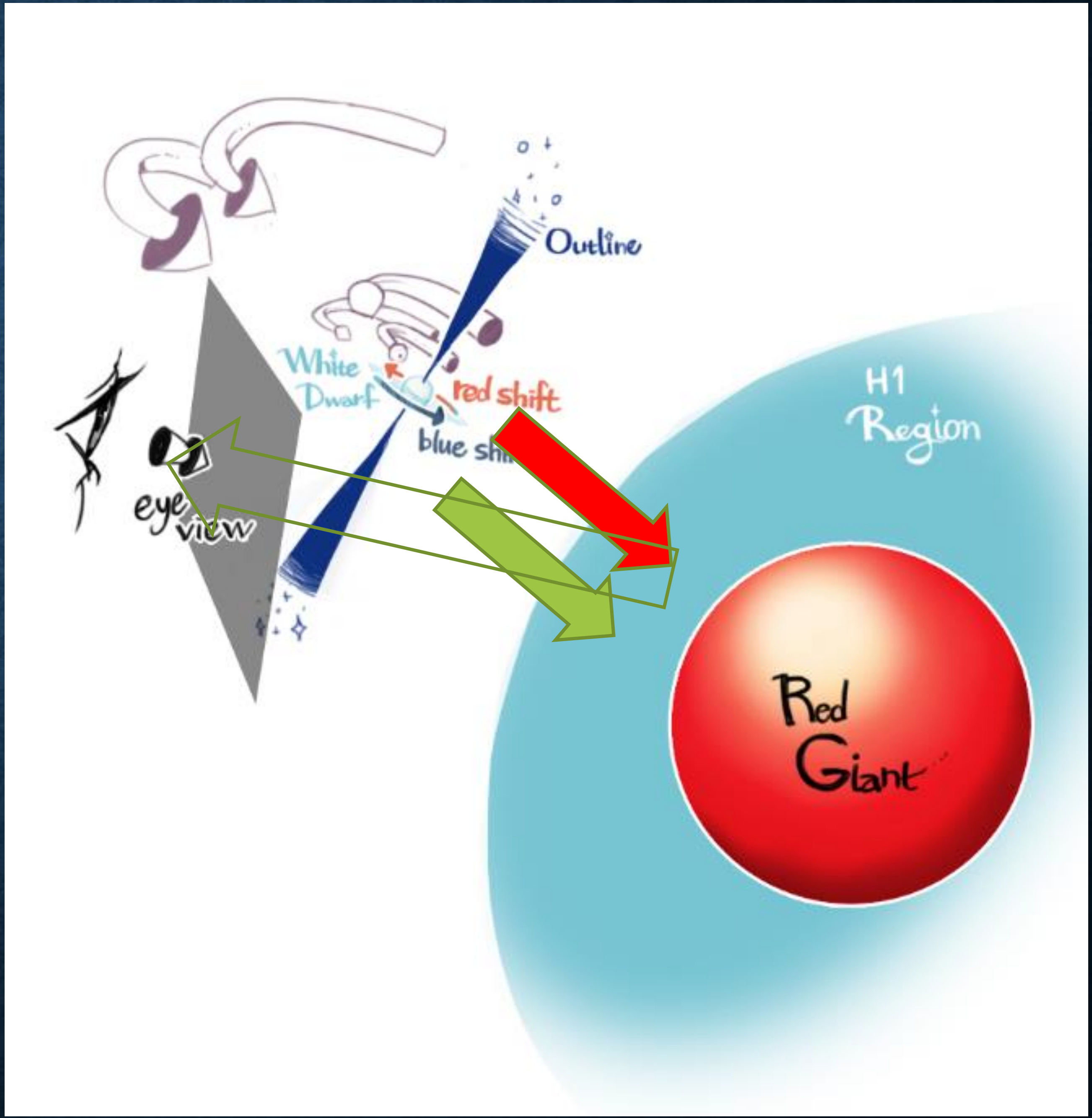

# POLARIZED RAMAN OVI IN SYMBIOTICS

1. Red wing part is polarized in the direction perpendicular to that of polarization of main part.
2. Polarization develops in the direction perpendicular to the scattering plane.
3. We need two scattering planes in order to explain the polarization of the main part and red wing part.
4. **An additional OVI or HI region in the direction perpendicular to the orbital plane moving away from the two stars.**

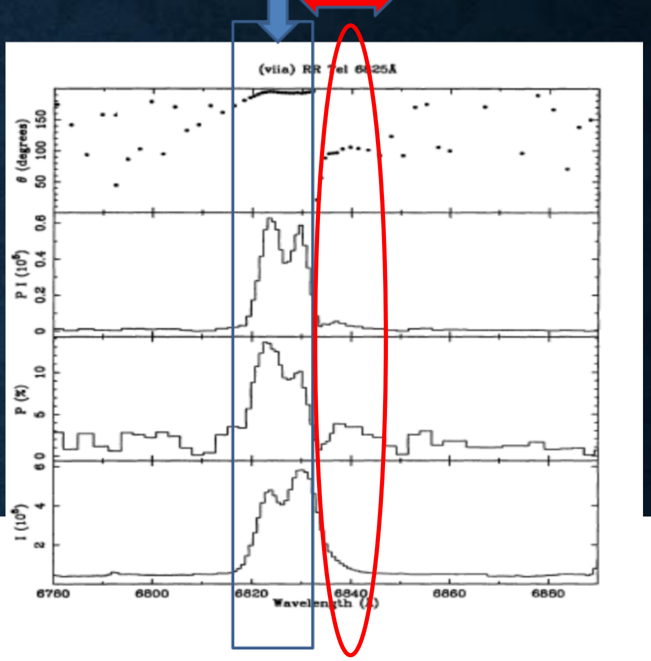


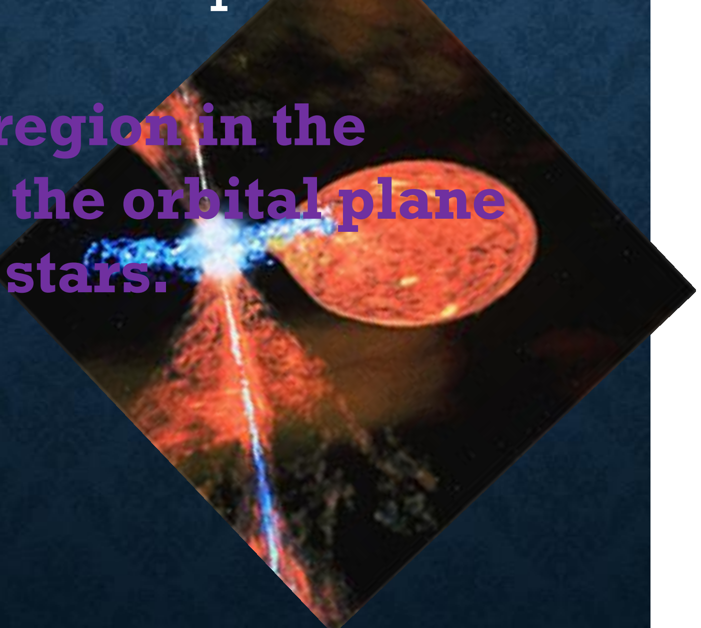

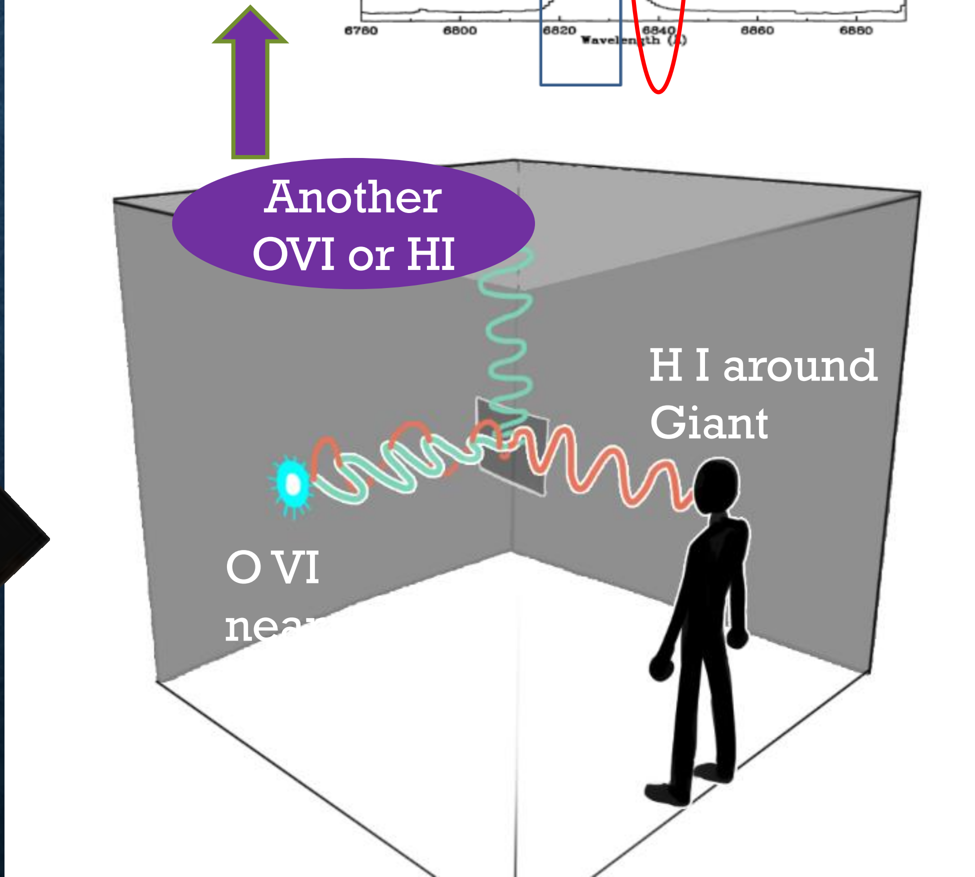

# MODELING OF POLARIZED RAMAN OVI

1. Asymmetric accretion flow + bipolar structure
2. OVI emission from a bipolar outflow?
3. Or additional HI regions receding in the bipolar direction?
4. Required conditions :

a) HI region subtends a substantial solid angle with respect to the O VI emission region.
b) Relative recession speed appears to be in the range ~ 50-100 km/s

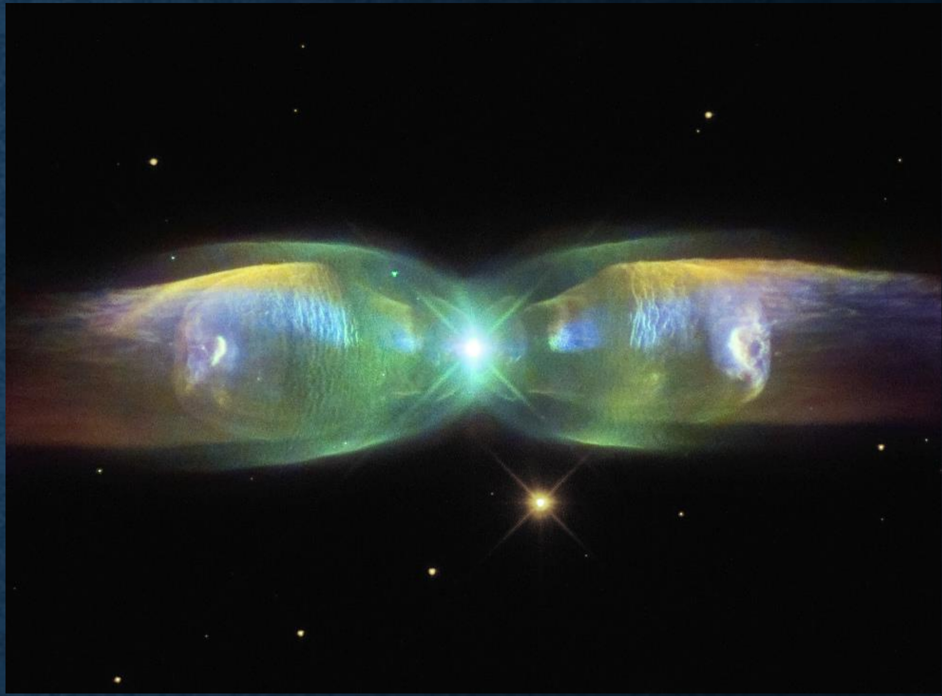

# SPECTROPOLARIMETRY OF SYMBIOTICS

1. Harries & Howarth (1996), H. M. Schmid
2. Double or Triple Peaks related to accretion and jet.
3. 7082 features are more strongly polarized than 6825.
4. S type symbiotics show stronger polarization than D types.
5. Polarization position angle varies according to the binary orbital motion → Works well for S type symbiotics, but noisy or poor with D type symbiotics

# AN ILLUSTRATED EXAMPLE M1-21

1. Triple peak structure in total flux and polarized flux for the 6825 feature.
2. Less well-discerned due to poor quality for the 7082 feature.
3. Strongest polarization appears in the blue peak.
4. Center peak appears to be contributed from the convergent side of the accretion flow and bipolar component.
5. Opposing polarizations cancel each other weakening polarization.

Red wing part exhbits flipped polarization.

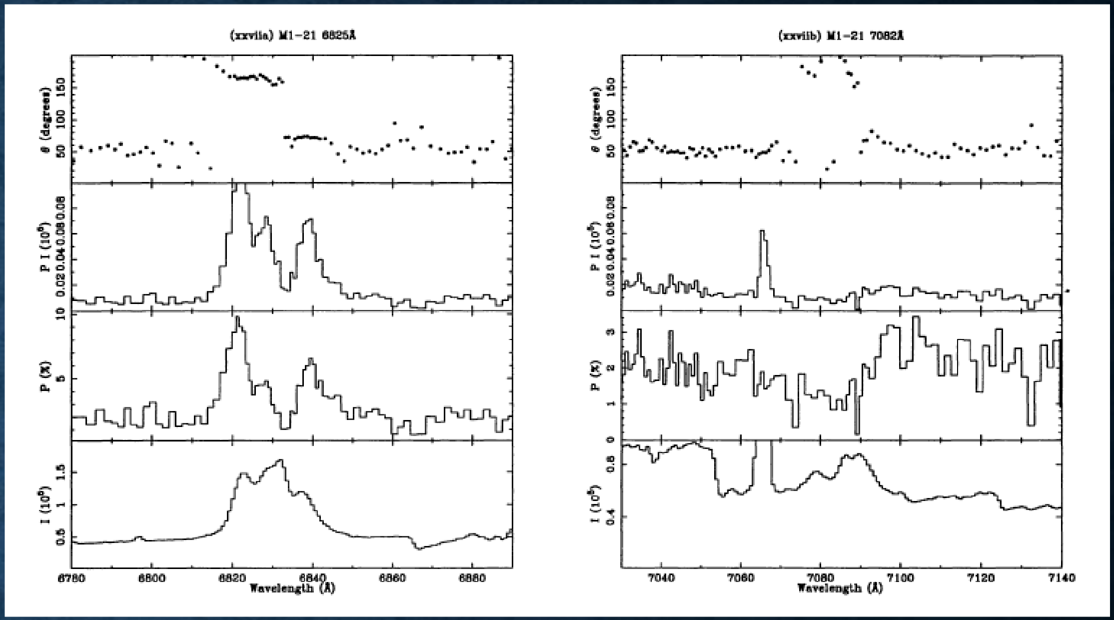


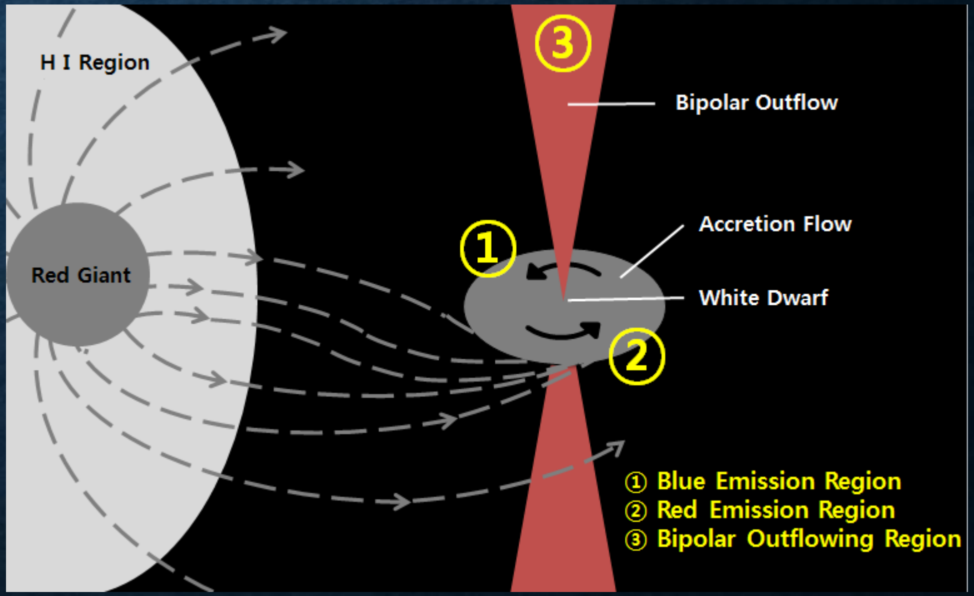

# CONCLUDING REMARKS

Raman O VI reveals tremendous amount of information regarding the accretion flow and bipolar outflows.
Should search more objects exhibiting  Raman OVI features. Narrow band filter survey may give us new objects waiting to tell us fascinating stories of the cosmos.  (Concalves, Akras)+(Angeloni, Heo, Chang)